

Dielectronic recombination in plasmas. II. Initial excited states

Gaber Omar

Physics Department, Ain Shams University, Abbasia, Cairo, Egypt

Yukap Hahn

Department of Physics, University of Connecticut, Storrs, Connecticut 06269

(Received 7 July 2000; published 27 March 2001)

Ions in a plasma recombine with electrons by both direct and resonant modes. The latter, the dielectronic recombination, can be a dominant process at temperature near $T \approx Z^2$ Ry, for ions with charge Z . The rates are usually given for target ions in their ground states, and contributions from all doubly excited intermediate states and final singly excited states of the recombined ions are summed over. To facilitate applications of the rates in plasma modelling in terms of rate equations, simple rate formulas are often devised. However, at finite temperature, a sizable fraction of ions is initially in an excited state, and after recombination, ions are usually left in singly excited final states. Thus new empirical rate formulas are needed that exhibit an explicit dependence on final as well as initial states of the ions before and after the recombination. We have calculated properly adjusted rates where (a) the target ions are allowed to be in their ground and excited states, and (b) contributions to the individual final states are explicitly separated. Multiple cascades are important in such calculations. For Al^{3+} ions we show that rates for the initial excited states are much larger than that for the ground state.

DOI: 10.1103/PhysRevE.63.046407

PACS number(s): 52.20.-j, 52.20.Fs, 34.80.Kw

I. INTRODUCTION

Dielectronic recombination (DR) rates are an important input parameter to rate equations that describe the time development of a plasma toward equilibrium. For given ionic species and at a specified temperature and density of free electrons and ions, population densities $N(n)$ of the final excited states n of the recombined ions are determined by rate equations which take into account all collisional transition effects on recombined ions by plasma electrons, as well as radiative cascades of the excited states. Presumably, the effect of plasma ionic field distortion on an actively participating central ionic system is included in the rates themselves. Evaluation of rates and the construction of rate equations must be coordinated in such a way that both these effects are properly incorporated, without double counting of their effects. The role of the rates and rate equations must be mutually complementary. This point was repeatedly stressed previously [1,2]; as the structure of rate equations change, corresponding rates must also be adjusted. To facilitate the use of the rates, calculated rates are fitted with parameters into a simple set of empirical rate formulas. It is important to note that generally the amount of benchmark calculations available is limited in quantity, with varying degrees of reliability. Therefore, the empirical formulas are useful not only in documenting the existing rates for ready applications, but also to extrapolate to cases (in T and Z) where data are not available. By including many sets of calculated data, the formulas can also adjust the overall reliability in some cases. The main concern of this report is the inadequacy of the existing rate formulas and the resulting inconsistencies in the plasma modeling.

A distinction must be made between studying a DR process that takes place in a plasma and another that is observed in collision experiments [3–7]. In the latter, one usually con-

trols the projectile energy e_c which must satisfy a resonance condition to reach a given intermediate resonance state R . The target is usually prepared initially in its ground state $i = g$, with the energy e_{ig} , in the process

$$e_{ci} + A^{Z+}(i) \rightarrow A^{ZM+}(R)^{**} \rightarrow A^{ZM+}(f)^* + x, \quad (1)$$

where the final singly excited states f are assumed to be Auger stable, and x denotes the radiation emitted during the second stage of process (1). For Auger-unstable final states j , further cascades may be needed to reach an Auger stable state f . In the following, we specify states f by the principal quantum number n . Detection of the process is then accomplished by observing the change in the ionic charge of the target after the recombination, from $Z+$ to $ZM+ = (Z-1)+$, or by measuring the energy of the x rays emitted. The cross section exhibits typical resonance peaks at e_{ci} that satisfy the resonance condition, $e_{ci} + e_{ii} = E_R$, where $R = (d_1 d_2)$ denote doubly excited resonance states of the recombined ion, with the energy approximately given by $E_R \approx e_{d1} + e_{d2}$. The cross sections for such an experiment are specified by g and R , but not necessarily by the final recombined states f , so that the final states f are usually summed over, under the assumption that eventually states f will radiatively relax to the ground state f_0 of the recombined ion. (The individual f 's are involved when e_x are measured.)

On the other hand, for the DR process in a plasma environment [8–10], free electrons with an assumed Boltzmann energy distribution are available, such that all the resonance states are allowed to contribute to the rates at the same time. Further, the initial states are not necessarily in the ground state g , and the final recombined states are not individually controllable as they are affected by the collisional effects of the plasma electrons. Since rate equations are usually constructed for a determination of the individual f states, and

their population distribution for the recombined ions, only the sum over resonance states R can be made, each with proper Boltzmann factors. The plasma collision effects on the final states f must then be treated by rate equations.

In part I of this series [11], we examined the problem of final state distribution. It was pointed out that modeling procedures commonly followed in the past employed the total DR rates only for the initial ground states $i=g$ of the target ions, and summed over contributions from all intermediate resonance states R and all singly excited states $f(n)$. The absence of the f dependence of the existing empirical formulas causes inconsistency, and it was proposed to correct the situation in part I. Thus an extended way of generating the DR rates was demonstrated in part I by an explicit calculation, and by retaining the dependence on the final states f , specifically for the Al^{3+} ions. It was assumed that the ions are initially in their ground states.

We should emphasize that there have been several notable exceptions to this unsatisfactory situation, in which the deficiency pointed out above was well recognized and the analyses were carried out by employing the calculated rates directly, rather than using the empirical rate formulas. However, comprehensive work to generate a complete set of improved rate formulas is yet to be carried out.

In the present paper, we carry the above extension further, and point out that the assumption adopted in most previous models, that the ions to be recombined are initially in their ground states, is also an oversimplification and again inconsistent with the rate equation approach. In fact, there are finite probabilities that the ions are initially in their excited states, and the DR can take place from these excited states. Since the excited states f for ions with $Z+$ logically become the initial states of ions with charge $(Z-1)+$ in the next stage of the modeling analysis, such a procedure is not self-consistent. We illustrate this problem by an explicit calculation of the corrected DR rates from the initial excited states (IES). Presumably, the IES, together with the final state distribution, may lead to serious changes in the determination of ionization balance.

Specification of both the initial and final states in the rates requires not only a large amount of computational effort in generating them, but also systematic ways to cataloging them in the form of rate formulas. The task is expected to be difficult, especially for DR modes that involve intershell excitations with multiple cascades. In fact, as previous studies [12–15] showed, resonance excitation from either ground or excited state targets produce a series of such final states, often with large cross sections, both for the $\Delta n' \neq 0$ and $\Delta n' = 0$ modes. The calculational procedure to be adopted in Sec. III for the specific target ion Al^{3+} is similar to that for the resonance excitation collisions; they are mutually complementary as the sum of their branching ratios should give unity.

II. RATE EQUATIONS AND DR RATES

Previous analyses of plasmas, modeling them in terms of rate equations, have shown that the excited state populations $N(n)$ of the recombined ions with $f=n>n_g$ can be substan-

tial, where n_g denotes the quantum number of the ground state of the recombined ion, and are sensitive functions of the electron temperature T and the free electron density N_e . In fact, most of the excited states with $n>n_{\text{SE}}$ reach Saha equilibrium (SE) values

$$N(n)^{\text{SE}} = n^2 (h^3/2\pi m k T)^{3/2} e^{J_n/kT} N_e N_+, \quad (2)$$

where J_n is the ionization energy of level n , and N_e and N_+ are the electron and ion densities, respectively. n_{SE} is the Saha n value, and is mildly T dependent; it usually assumes a value between 10 and 20. At fixed T , the excited state population $N(n+1)$, as compared with $N(n)$, is roughly proportional to the Boltzmann factor; i.e., $r(n) = N(n+1)/N(n) = \exp(-\Delta_n/kT)$, showing the sensitivity of the ratio on T , where $\Delta_n = e_{n+1} - e_n > 0$. However, it was also found that most excited states with n in the range $n_{\text{SE}} > n > n_B$ quickly reach values close to that of Saha, where the bottleneck n_B usually assumes the value around 4 or 5, and $n_B \ll n_{\text{SE}}$. On the other hand, for $n < n_B$, the final $N(n)$ are usually much larger than the Saha values, and are determined by the solution of the rate equations. For example, in hydrogen plasmas, the equilibrium population for the ground states is about four times the Saha value [9]. The ratios $r(n)$ at equilibrium are also sensitive to the continuum electron density N_e ; at $N_e \approx 10^{15} \text{ cm}^{-3}$ we have $r(g) \approx 0.3$, while at $N_e \approx 10^{18} \text{ cm}^{-3}$ r increases to $r(g) \approx 1$. This latter number implies that the ground and first excited state populations are of the same magnitude. For a transient plasma [16], where N_+ and N_e are allowed to vary during the relaxation, these effects are even more dramatic, as the population of the continuum electrons changes rapidly during the time period of order $\Delta t \approx 10^{-10}$ to 10^{-8} sec.

The rate equations for the final state density $N(n)$, as conventionally formulated, are

$$\begin{aligned} dN(n)/dt = & - \left(N_e C_n^I + N_e \sum_{n' \neq n} C_{nn'}^X + \sum_{n' < n} A_{nn'} \right) N(n) \\ & + \left(N_e \sum_{n' \neq n} C_{n'n}^X + \sum_{n' > n} A_{n'n} \right) N(n') \\ & + N_e N_+ \alpha_n, \end{aligned} \quad (3)$$

where C^I and C^X are the collisional ionization and excitation-deexcitation rates, respectively, and the A 's are the radiative decay rates. The last term in Eq. (3) contains the recombination rates, as

$$\alpha_n = \alpha_n^{\text{RR}} + \alpha_n^{\text{TBR}} + \alpha_n^{\text{DR}} \quad (4)$$

for radiative recombination (RR) and three-body recombination (TBR), and the last term for DR, all to the final states n . The crucial point of the discussion here is that the ion density N_+ in Eq. (3) and the rates in Eq. (4) are for the ground state of the ions of charge Z before capture.

What is being proposed here is not new, as several previous works on modeling already recognized the need. However, no comprehensive work in generating the necessary rates has been carried out. Furthermore, as stressed in Sec. I,

the structure of the rates should reflect the particular rate equations one constructs and to which the rates are inserted. As the modeling equations are refined, more detailed information must be carried by the rate equations, in a consistent way without double counting. That is, the effect of the states omitted in a particular set of rate equations must be included in the corresponding rates, and vice versa. Thus the desired adjustment involves, for example, replacement of the last DR term in Eq. (3) with Eq. (4) by a more general form

$$d(\Delta N(n))/dt = +N_e \left[N_{+g} \alpha_{ng} + \sum_{i \neq g} N_{+i} \alpha_{ni} \right], \quad (5)$$

where the subscript i denotes the excited states of the target ions before capture. The rates α^{DR} , with $i=g$ and $i=1,2,3,\dots$, are defined, in terms of A_a and A_r , as

$$\begin{aligned} \alpha^{DR}(i \rightarrow R \rightarrow f) \\ = (4\pi R y / kT)^{3/2} (g_R / 2g_i) \exp(-e_{ci} / kT) \\ \times A_a(R \rightarrow c, i) A_r(R \rightarrow f) / (\Gamma_a + \Gamma_r), \end{aligned} \quad (6)$$

where the subscripts r and a represent the radiative and auto-ionization processes, respectively, and where the Γ 's are the total rates defined by $\Gamma_a = \sum_i A_a(R \rightarrow i)$ and $\Gamma_r = \sum_k A_r(R \rightarrow k)$. The rates of interest are then given by

$$\alpha_{ni}^{DR} = \sum_R \alpha^{DR}(i \rightarrow R \rightarrow f), \quad (7)$$

where $f=f(n)$ and the dependence on Z and T are implicit. Evidently, tabulation of such quantities which depend on the both IES in terms of i and final state distribution in terms of $f=n$ at many different temperatures and charge states will be very complex but required.

We further clarify the necessity of introducing the IES in the rate equation analysis. The modeling is conducted by solving a set of rate equations for the excited state density $N(n)$, for a pair of charge states at a time, say the target ion with charge $Z+$ and the recombined ions with charge $ZM + = (Z-1)+$. Thus the analysis starts from $Z=Z_C$ nuclear core charge of the ion, producing the recombined ions of charge Z_C-1 . Next, the ions with charge Z_C-1 are the targets, producing ions with Z_C-2 by recombination, etc. This process will continue until Z reaches 1 as a target, and producing neutral atoms. In each case involving a charge pair, the equilibrium distribution of the ground and excited state populations of the recombined ions are calculated as functions of temperature. Therefore, for any given Z , there will be a finite probability of having excited states, which should form the starting point of the next stage in Z . In almost all cases treated previously, the simplifying approximation of neglecting the IES has been made and only the ground state g kept. This applies not only to DR rates, but also to RR and TBR rates as well. Independent of whether such modifications can make a sizable difference in the final solutions, it is important to recognize the inconsistencies of

such approaches, the validity of which is density and temperature dependent, and must be checked on a case by case basis.

An approximate set of rate equations for the final excited state distribution $N(n)$ of the recombined ions is usually set up such that only the principal quantum number n of $f=(n,l)$ is explicitly retained. Then the input rates must be adjusted to this by directly summing over l . Similarly, if the rate equations contain only the N_{Z,n_i} , then contributions to the rates from different l_i of the initial states $i=(n_i, l_i)$ may be averaged over, in order to obtain α_{n,n_i} . Here, with the weight $(2l_i+1)$, we have

$$\alpha_{n,n_i}^{DR} \equiv \sum_{l_i} (2l_i+1) \alpha_{n,n_i,l_i}^{DR} / n_i^2. \quad (8)$$

III. DR RATES FOR INITIAL EXCITED STATES

Calculation of DR rates for initial excited states of the target ions is complicated because of many cascade steps that are often involved in reaching the singly excited final states of the recombined ions. In order to reduce the complexity of the calculation to a manageable level, in the following we adopt a set of simplifying approximations; the isolated resonance approximation, angular momentum average coupling scheme, and single configuration Hartree-Fock and distorted wave approximation for the bound and continuum orbitals. Dependence of the rates on IES and final excited states is included.

The DR rates for the Ne-like Al^{3+} with IES are calculated. To simplify notation, reference to the spectator core electrons $1s^2 2s^2$ is omitted from the initial (I 's), resonance (R 's) and final (f 's) states. They are explicitly included during the generation of wave functions and energies of the active electrons involved in the reaction. We denote the three allowed IES for the Ne-like ions as I_1 , I_2 , and I_3 for $2p^5 3s$, $2p^5 3p$, and $2p^5 3d$, respectively, while the initial ground state is $g=2p^6$.

Group A ($2p^5 3snl$) of resonance states R may be formed only from the g state and not from any of the other IES. They are the dominant states that contribute to the individual final states, as discussed previously in part I. The initial state I_1 creates R states of groups B ($2p^5 3pnl$) and C ($2p^5 3dnl$). But I_2 produces only group C . On the other hand, I_3 can go to R states of group D ($2p^5 4lnl$) only, while group D may also be reached from I_1 , I_2 and g . The DR rates for group D with g as initial state are very small, as shown in part I but relatively large for the other IES. Thus, group D states were neglected in part I but are included here.

In Table I we present the DR rates for the IES equivalent to I_1 , and they are compared with that obtained for the initial ground state g . For many R , the rates with I_1 are much larger than that with g ; e.g., for $R=2p^5 3d4s$ and $R=2p^5 3d4f$, the rates with I_1 are 92 and 175 times larger than that with g . We present the result only for $R=2p^5 3p5s$ and $2p^5 3p5d$ from group B , because all the other R states ($2p^5 3pnl$ with $n>4$) give small DR rates. In addition, state I_1 is energetically unable to reach $R=2p^5 3p4l$. We also present the rates

TABLE I. The final state distribution of the DR rates is given for the two different initial states $I_0 = g \equiv 2p^6$ and $I_1 \equiv 2p^5 3s$. All the rates are given in units of $10^{-14} \text{ cm}^3/\text{sec}$; numbers in square brackets are powers to 10 in addition to -14 . For example, $2.0 [-3]$ means 2.0×10^{-17} . Many other small rates associated with the intermediate states $3pnl$ are omitted from the table.

R	f I	$n=3$			$n=4$				$n=5$				
		$3s$	$3p$	$3d$	$4s$	$4p$	$4d$	$4f$	$5s$	$5p$	$5d$	$5f$	$5g$
$3p5s$	g	8.1[-5]	2.0[-3]						9.5[-4]				
	I_1	5.4[-3]	1.4[-1]						6.3[-2]				
$3p5d$	g	6.1[-5]	3.8[-2]								3.5[-3]		
	I_1	2.1[-3]	1.32								1.2[-2]		
$3d4s$	g		6.0[-5]	5.2[-3]	2.6[-2]								
	I_1		5.6[-3]	4.8[-1]	2.41								
$3d4p$	g	7.4[-6]		7.2[-5]	4.4[-6]	2.8[-1]							
	I_1	1.9[-4]		1.7[-3]	1.1[-4]	6.93							
$3d4d$	g	5.1[-6]	2.3[-3]	6.6[-1]			3.5						
	I_1	1.5[-5]	6.7[-3]	1.98			10.2						
$3d4f$	g			1.2[-4]				7.8[-2]					
	I_1			2.2[-2]				13.7					
$3d5s$	g		5.9[-6]	4.7[-4]		3.4[-5]			7.8[-2]				
	I_1		4.1[-4]	3.1[-2]		2.3[-3]			5.2[-1]				
$3d5p$	g			2.9[-6]			3.7[-6]			2.8[-2]			
	I_1			6.1[-5]			7.8[-5]			5.9[-1]			
$3d6d$	g		1.6[-4]	2.7[-2]				7.3[-5]			2.5[-1]		
	I_1		4.2[-4]	6.8[-2]				1.9[-4]			6.4[-1]		
$3d5f$	g		2.1[-5]	4.4[-6]			2.5[-6]					6.9[-3]	
	I_1		2.4[-3]	5.0[-4]			2.8[-4]					7.8[-1]	
$3d5g$	g							6.4[-6]					8.6[-4]
	I_1							6.7[-3]					8.7[-1]
subtot	g		0.74				3.9				0.37		
	I_1		4.1				33.2				3.5		

for the R states of group C with $n=4$ and $n=5$, i.e., $2p^5 3d4l$ and $2p^5 3d5l$. The drastic decrease in DR rates, from $33.2[-14]$ to only $3.5[-14] \text{ cm}^3/\text{sec}$, for $n=4$ and 5 , may be attributed to the Auger channel to I_2 which is allowed for the $n=5$ state, but not for $n=4$. Consequently, the total resonance widths $\Gamma(R)$ increase while the fluorescence yields ω 's decrease for $n=5$. For $n>5$, no new decay channels other than that lead to g , I_1 and I_2 occur for group C . Hence the HRS contributions to the total DR rates from group C can be safely estimated from the rates at $n=5$ using the n^{-3} scaling. The monotonic increase of DR rates with the orbital quantum number l of the final excited states of $n=4$ and 5 is noted (Table I). However, we expect the rates to decrease at higher l . Of course, the n and l dependence of the rates is not apparent once all the contributions are summed, as has been done in the past.

In Table II, we present the DR rates with I_2 as the initial excited state. In this case, only the R states from group C dominate; specifically, $R=3dnl$, with $n=5$ and 6 , is considered, where n is also the principal quantum number of the singly excited final states f . It is found that the Auger rate for $C \rightarrow I_2$ is at least ten times larger than that for $C \rightarrow I_1$, but 100 times of that to the ground g state for $R=2p^5 3d5p$. That is, $\Gamma_a = \sum A_a(R \rightarrow g)$, $A_a(R \rightarrow I_1)$ and $A_a(R \rightarrow I_2)$ have the values $0.259[12]$, $0.11[14]$, and $0.146(15) \text{ scc}^{-1}$, respec-

tively, and thus we have a large capture probability $V_a(I_2 \rightarrow R)$. Overall, the DR rates from group C states with initial I_2 are very large relative to those with I_1 and g . The small rates for $n=3$ in Table I and $n=3$ and 4 in Table II are caused by multistep cascade decays and not by direct radiative decay of R states.

The rates $\alpha^{\text{DR}}(g \rightarrow R \rightarrow f)$ are also presented for comparison with $\alpha^{\text{DR}}(I_2 \rightarrow R \rightarrow f)$ for each individual R state. As it is clear from the table, the DR rates with g and I_2 are not in a constant ratio as we go to different R states, e.g., $\alpha^{\text{DR}}(I_2)/\alpha^{\text{DR}}(g)=90$ for $R=2p^5 3d5p$, but this ratio drops to only 17 for $R=2p^5 3d5d$. Such variation precludes the possibility of estimating rates for the IES from that for g .

The DR rates for group D ($4lnl$) of resonance states R are presented in Table III. As previously mentioned, $4lnl$ states may be formed from g or any of the three IES. There are four rows of α^{DR} in the table for each R state, corresponding to the initial states g , I_1 , I_2 , and I_3 . This table is useful for comparing the rates for different IES. Clearly, the DR rates for group D are very small in the case of the initial ground state g . Thus, group D was neglected in part I of this study, where the focus was on the final state distribution, from the initial state g . Note that the $R=4snl$ resonance states are not allowed to be formed from $I_3=2p^5 3d$, because $4s$ orbital lies energetically below the $3d$ orbital. The states R

TABLE II. Same as in Table I, but for the initial excited state $I_2 \equiv 2p^5 3p$. The DR rates are presented and compared with values obtained for the initial g state.

d	f	$n=3$			$n=4$			$n=5$			$n=6$						
		l	$3p$	$3d$	$4p$	$4d$	$4f$	$5s$	$5p$	$5d$	$5f$	$5g$	$6s$	$6p$	$6d$	$6f$	$6g$
$3d5s$	g	5.9[-6]	4.7[-6]	3.4[-6]			7.8[-3]										
	I_2	6.9[-4]	5.5[-2]	4.0[-4]			9.1[-1]										
$3d5p$	g		2.9[-6]		3.7[-6]			2.8[-2]									
	I_2		2.6[-4]		3.3[-4]			2.53									
$3d5d$	g	1.6[-4]	2.7[-2]				7.3[-5]		2.5[-1]								
	I_2	2.7[-3]	4.5[-1]				1.2[-3]		4.21								
$3d5f$	g	2.1[-5]	4.4[-6]			2.5[-6]				6.9[-3]							
	I_2	3.3[-4]	3.4[-3]			1.9[-3]				5.22							
$3d5g$	g						6.5[-6]				8.6[-4]						
	I_2						5.7[-2]				7.68						
$3d6s$	g	3.1[-6]	2.6[-4]	1.4[-6]				2.9[-6]				6.5[-3]					
	I_2	3.6[-4]	3.2[-2]	1.6[-4]				3.4[-4]				7.6[-1]					
$3d6p$	g		1.9[-6]		1.3[-6]				2.7[-6]				2.7[-2]				
	I_2		1.7[-4]		1.1[-4]				2.4[-4]				2.41				
$3d6d$	g	1.4[-4]	1.5[-2]				2.1[-5]			5.9[-5]				2.1[-1]			
	I_2	2.5[-3]	2.4[-1]				3.2[-4]			9.4[-4]				3.42			
$3d6f$	g		2.2[-6]		1.1[-6]				7.1[-6]						6.6[-3]		
	I_2		1.2[-3]		5.8[-4]				3.8[-3]						3.54		
$3d6g$	g						5.7[-6]			4.3[-6]							5.1[-4]
	I_2						1.2[-2]			9.2[-3]							6.61
Subtot	g		4.0[-1]			1.2[-4]			2.9[-1]					2.6[-1]			
	I_2		0.8			6.3[-1]			20.6					16.7			

$=2p^5 4p4d$ cannot be formed from I_3 (marked by dashes). On the other hand, $R=2p^5 4pnl$ may be formed from I_3 for $n \geq 5$, but the corresponding rates are small. However, all the states $R=2p^5 4dnl$ and $2p^5 4fnl$ are produced from I_3 for $n > 3$, and give large rates, but smaller than that for I_2 produced by group C in Table II. From Tables I–III, we conclude that the DR rates for $I_2=2p^5 3p$ are the largest, relative to other initial excited states and the ground state.

In Table IV, we present the final state distribution of α^{DR} for $R=2p^5 3d5d$, and stress the following three points: (i) At a temperature of 3.7 Ry, we have $\alpha^{\text{DR}}(I_2)/\alpha^{\text{DR}}(I_1)=6.6$ and $\alpha^{\text{DR}}(I_2)/\alpha^{\text{DR}}(g)=17$. That is, the DR rates for I_2 is again the largest. (ii) With I_2 and at two temperatures, 0.22 and 3.7 Ry, we have

$$\alpha^{\text{DR}}(I_2, kT=0.22 \text{ Ry})/\alpha^{\text{DR}}(I_2, kT=3.7 \text{ Ry})=17, \quad (9)$$

indicating that with IES, the DR rates increase dramatically at low temperature. This is as expected, because of small excitation energies involved with IES. (iii) The ratio between the maximum DR rates for I_2 and g initial states is found to be

$$\begin{aligned} & \alpha^{\text{DR}}(I_2, kT=0.22 \text{ Ry, max})/\alpha^{\text{DR}}(g, kT=3.7 \text{ Ry, max}) \\ & = 289, \end{aligned} \quad (10)$$

where $kT=3.7 \text{ Ry}=\frac{2}{3}e_{cg}(g)$ and $kT=0.22 \text{ Ry}=\frac{2}{3}e_{c2}(I_2)$.

Next, we examine the effect of the initial excitation modes involving the $2p$ or $3s$ electrons in I_1 , for example. The two different excitation modes are

$$2p^5 3s + e_1 \rightarrow 2p^4 3s 3d 4d \quad (R1) \quad (2p \rightarrow 3d), \quad (11a)$$

$$2p^5 3s + e_2 \rightarrow 2p^5 3d 4d \quad (R2) \quad (3s \rightarrow 3d). \quad (11b)$$

The DR rates are calculated at the same temperature, $kT=3.7 \text{ Ry}$ for the two processes. The final state distribution of DR rates for $R1$ and $R2$ are presented in Table V. It is found that the rates are very small for $R1$, while the rates for $2p^6 3d$ and $2p^6 4d$ from $R2$ are 100 times larger than that from $R1$. The $2p$ excitation is not important for Ne-like ions when $2p^5 3s$ is the initial excited state, and, at low temperature, $kT=0.44 \text{ Ry}$, the DR rates for $R2$ have increased by almost a factor of 7. This is consistent with the trend in T observed in Table IV, that the rates with IES are large at low T . The ratio between maximum DR rates for $R2$ and $R1$ are calculated at $kT=\frac{2}{3}e_{c2}=0.44 \text{ Ry}$ and $kT=\frac{2}{3}e_{c1}=5.2 \text{ Ry}$, respectively, where e_{c1} and e_{c2} represent the continuum electron energies corresponding to $R1$ and $R2$ when they are formed from same initial excited state, $I_1=2p^5 3s$. It is found that

$$\alpha^{\text{DR}}(R2, \text{max}, 0.44 \text{ Ry})/\alpha^{\text{DR}}(R1, \text{max}, 5.2 \text{ Ry})=2.3 \times 10^3. \quad (12)$$

TABLE III. The DR rates group $D(4lnl')$ resonance states and for the three initial excited states I_1 , I_2 , and I_3 are presented and compared with that for the ground state g . The intermediate states $2p^5 4snl$ cannot be created from $I_3=2p^5 3d$, so that its contribution is absent.

R	f I	$n=3$				$n=4$			$n=5$				
		$3s$	$3p$	$3d$	$4s$	$4p$	$4d$	$4f$	$5s$	$5p$	$5d$	$5f$	$5g$
$4p4d$	g	6.4[-6]		8.7[-7]		2.0[-2]	1.9[-5]						
	I_1	4.9[-5]		6.7[-6]		1.5[-1]	1.5[-4]						
	I_2	3.2[-4]		4.4[-5]		9.7[-1]	1.1[-3]						
	I_3	----		----		----	----						
$4d2$	g	2.5[-10]		3.4[-11]		7.6[-7]	2.1[-2]						
	I_1	2.8[-10]		3.8[-11]		8.1[-7]	2.4[-2]						
	I_2	1.8[-9]		2.4[-10]		5.1[-6]	1.4[-1]						
	I_3	1.2[-8]		1.5[-9]		3.4[-5]	9.6[-1]						
$4d4f$	g			8.4[-8]			4.4[-7]	3.3[-3]					
	I_1			1.9[-6]			1.1[-5]	7.8[-2]					
	I_2			3.4[-6]			1.8[-5]	1.4[-1]					
	I_3			4.5[-5]			2.3[-4]	1.76					
$4d5s$	g		4.5[-6]			5.9[-8]	5.8[-4]		3.2[-3]				
	I_1		2.6[-4]			3.5[-6]	3.4[-2]		1.8[-1]				
	I_2		4.3[-5]			5.1[-7]	5.6[-3]		3.1[-2]				
	I_3		3.1[-3]			3.9[-6]	3.6[-2]		2.0[-1]				
$4d5d$	g		1.6[-6]				7.8[-3]	6.0[-9]			2.6[-2]		
	I_1		1.4[-6]				7.1[-3]	5.5[-9]			2.4[-2]		
	I_2		5.4[-6]				2.7[-2]	2.1[-8]			8.8[-2]		
	I_3		7.8[-5]				3.8[-1]	2.0[-7]			1.26		
subtot	g		1.3[-5]			5.3[-2]				2.9[-2]			
	I_1		3.2[-4]			2.9[-1]				2.0[-1]			
	I_2		4.3[-4]			1.28				1.2[-1]			
	I_3		3.2[-3]			3.14				1.46			

Thus, the $3s$ excitation has DR rates two or more thousands times larger than $2p$ excitation, when the reaction starts from the initial excited state. In general, it is concluded from Tables IV and V that DR rates are huge if the target is in any singly excited state relative to that of target in its ground state, especially at low temperatures.

In order to illustrate the complexity of calculating the rates with IES and multiple cascades, a typical case is presented in the Appendix, where most of the important intermediate states are explicitly included.

TABLE IV. The DR rates for the initial excited state $I_2 = 2p^5 3p$ at two different temperatures $kT=0.22$ and 3.7 Ry are presented, in order to illustrate the temperature dependence. The resonance state $R=2p^5 3d4d$ is chosen for this purpose. The rates are compared with that for I_1 and g initial states for the same R .

Initial states	Final excited states				kT (Ry)
	$3p$	$3d$	$4f$	$5d$	
$g=2p^6$	1.6[-4]	2.7[-2]	7.3[-5]	2.5[-1]	3.7
$I_1=2p^5 3s$	4.2[-4]	6.8[-2]	1.9[-4]	6.4[-1]	3.7
$I_2=2p^5 3p$	2.7[-3]	4.5[-1]	1.2[-3]	4.2	3.7
$I_2=2p^5 3p$	4.6[-2]	7.6	2.1[-2]	71.6	0.22

IV. SUMMARY

The present study completes the two important adjustments on the DR rates that are needed to make the plasma modelling analyses self consistent. As discussed in part I the final recombined state dependence of the rates as represented by α_n^{DR} are important in the construction of the rate equations. This problem is peculiar to the current status of the available DR rates, because most of the other processes are treated correctly in the sense that the final as well as the initial states are properly specified. Second, as discussed in the present paper, the initial target ions that undergo recom-

TABLE V. The DR rates are given for the same initial state $I_1 = 2p^5 3s$ but forming two different intermediate states $R1$ and $R2$ resonance states defined in Eq. (11) by exciting the $2p$ and $3s$ electrons of the target ion, respectively.

Resonance (R) states	Final excited states				kT (Ry)
	$3s$	$3p$	$3d$	$4d$	
$R1=2p^4 3s 3d 4d$	1.3[-2]	7.6[-6]	2.0[-3]	2.8[-2]	5.2
$R1=2p^4 3s 3d 4d$	1.2[-2]	7.0[-6]	1.8[-3]	2.5[-2]	3.7
$R2=2p^5 3d 4d$	1.5[-5]	6.7[-3]	1.98	10.2	3.7
$R2=2p^5 3d 4d$	9.9[-5]	4.4[-2]	12.5	64.8	0.44

ination need not be all in their ground states. This is represented by the dependence of the rates on the index $i = g, 1, 2, \dots$, as α_{ni}^{DR} , where the final states are given in terms of the quantum number n . We have shown by detailed calculation that the rates from the initial excited states are in general very large, often by as much as a factor of 10. Incidentally, in so far as IES are concerned, none of the existing recombination rates have this point taken into account; this is the situation for the DR rates as well as for the radiative and three-body recombinations.

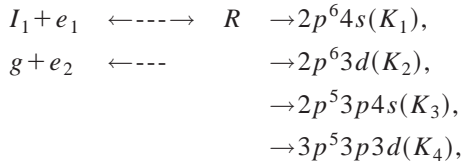
As noted in Sec. I, the resonance excitation automatically specifies the initial and final state dependence. Therefore, the calculation of DR with both the initial and final states specified is similar to that for the resonant excitation process. On the other hand, the present study does not include the effect of the plasma microfield, although they can be very important. Actual use of new modified rates in the modeling must wait until enough of the rates with IES become available. How serious the effects of these changes in the rates on plasma modeling are is yet to be examined.

ACKNOWLEDGMENTS

This work was supported in part by the Egyptian Cultural Bureau in the U.S., and by the University of Connecticut. G.O. would like to thank the Physics Department of the University of Connecticut for hospitality and use of the computer facility.

APPENDIX: AN EXAMPLE OF DR RATES WITH IES

Consider a target ion in the initial excited state $I_1 = 2p^5 3s$, which collides with free electrons, and the resonance state $R = 2p^5 3d 4s$ is formed. This R state will decay as follows:



where g is the ground state, $g = 2p^6$, obtained from R by Auger decay, and the states $K_1 - K_4$ are reached from R by radiative decays. The values of continuum energies corresponding to I_1 and g are $e_1 = 0.3$ Ry and $e_2 = 6.1$ Ry. The values of Auger rates are, $A_a(R \rightarrow I_1) = 0.1281$ [15] and $A_a(R \rightarrow g) = 0.5551$ [12] sec^{-1} , while the radiative rates are $A_r(R \rightarrow K_1, K_2, K_3 \text{ and } K_4)$ are 0.5635 [10], 0.1128 [10], 0.1975 [10], and 0.6019 [10] sec^{-1} , respectively. Accordingly, the capture probability $V_0(I_1 \rightarrow R) = 0.6406(15) \text{sec}^{-1}$. The final singly excited states K_1 and K_2 are Auger stable, having fluorescence yields, $\omega(R \rightarrow K_1) = 0.437$ [−4] and $\omega(R \rightarrow K_2) = 0.87$ [−5], respectively. Thus, at $kT = 3.7$ Ry, the DR rates for K_1 and K_2 are

$$\alpha^{\text{DR}}(I_1 \rightarrow R \rightarrow K_1) = 2.41[-14] \text{ cm}^3/\text{sec} \quad (\text{A1})$$

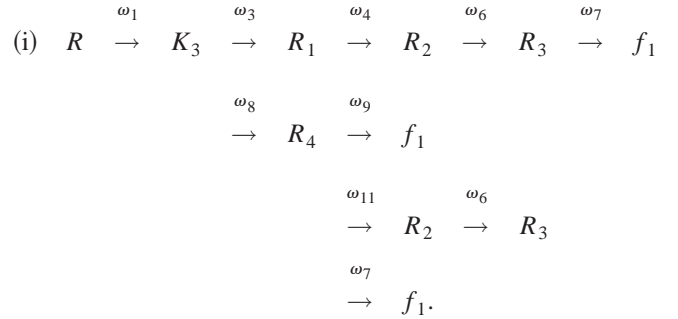
and

TABLE VI. Values of the fluorescence yields ω 's for the intermediate states which appear during the cascade decay of $R = 2p^5 3d 4s$, ending in the final singly excited f . They are used in the example given in the Appendix.

i	Transition	ω_i	i	Transition	ω_i
1	$R \rightarrow K_3$	0.153[−4]	10	$R_4 \rightarrow f_4$	0.201
2	$K_3 \rightarrow f_2$	0.48[−3]	11	$R_4 \rightarrow R_2$	0.119
3	$K_3 \rightarrow R_1$	0.62[−3]	12	$R \rightarrow K_4$	0.47[−4]
4	$R_1 \rightarrow R_2$	0.115[−2]	13	$K_4 \rightarrow f_2$	0.20[−2]
5	$R_2 \rightarrow f_2$	0.59[−3]	14	$K_4 \rightarrow R_1$	0.69[−3]
6	$R_2 \rightarrow R_3$	0.31[−4]	15	$K_4 \rightarrow R_5$	0.34[−3]
7	$R_3 \rightarrow f_1$	0.26[−1]	16	$R_5 \rightarrow f_1$	0.22[−2]
8	$K_3 \rightarrow R_4$	0.30[−3]	17	$R_5 \rightarrow f_3$	0.19[−2]
9	$R_4 \rightarrow f_1$	0.42[−1]	18	$R_5 \rightarrow R_2$	0.116[−2]

$$\alpha^{\text{DR}}(I_1 \rightarrow R \rightarrow K_2) = 0.48[-14] \text{ cm}^3/\text{sec} \quad (\text{A2})$$

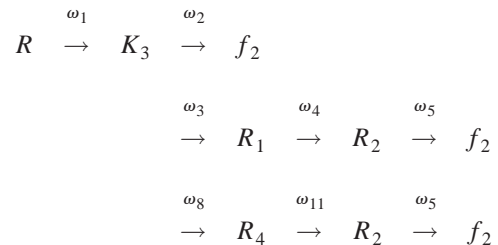
However, K_3 and K_4 are still Auger unstable, and cascade decay to reach the singly excited states $f_1 = 2p^6 3s$, $f_2 = 2p^6 3p$, $f_3 = K_2 = 2p^6 3d$, and $f_4 = K_1 = 2p^6 4s$. In fact, the cascade decays of K_3 and K_4 pass, in many ways, through the transient resonances $R_1 = 2p^5 3p^2$, $R_2 = 2p^5 3s 3p$, $R_3 = 2p^5 3s^2$, $R_4 = 2p^5 3s 4s$, and $R_5 = 2p^5 3s 3d$. The fluorescence yields ω 's for the cascade decays are presented in Table VI. For example, the final excited state f_1 may be generated from K_3 as follows



Thus, $\omega(R \rightarrow K_3 \rightarrow f_1) = \omega_1 x (\omega_3 x \omega_4 x \omega_6 x \omega_7 + \omega_8 x \omega_9 + \omega_8 x \omega_{11} x \omega_6 x \omega_7) = 0.194$ [−9], resulting in the rates

$$\alpha^{\text{DR}}(R \rightarrow K_3 \rightarrow f_1) = 0.107[-18] \text{ cm}^3/\text{sec}. \quad (\text{A3})$$

(ii) The state f_2 is reached from K_3 as



Consequently, $\omega(R \rightarrow K_3 \rightarrow f_2) = \omega_1 (\omega_2 + \omega_3 x \omega_4 x \omega_5 + \omega_8 x \omega_{11} x \omega_5) = 0.735$ [−8], and thus

$$\alpha^{\text{DR}}(R \rightarrow K_3 \rightarrow f_2) = 0.405[-17] \text{ cm}^3/\text{sec}. \quad (\text{A4})$$

(iii) The state f_4 is reached from K_3 as

$$R \xrightarrow{\omega_1} K_3 \xrightarrow{\omega_8} R_4 \xrightarrow{\omega_{10}} f_4$$

and thus $\omega(R \rightarrow K_3 \rightarrow f_4) = \omega_1 x \omega_8 x \omega_{10} = 0.923[-9]$. We then have

$$\alpha^{\text{DR}}(R \rightarrow K_3 \rightarrow f_4) = 0.509[-18] \text{ cm}^3/\text{sec}. \quad (\text{A5})$$

In addition, the state K_4 may lead finally to f_1 , f_2 , and f_3 by various routes through the transient states as follows.

(iv) The state f_1 from K_4 :

$$\begin{array}{ccccccccc} \omega_{12} & & \omega_{14} & & \omega_6 & & \omega_7 & & \\ R & \rightarrow & K_4 & \rightarrow & R_1 & \rightarrow & R_3 & \rightarrow & f_1 \\ & & & & & & & & \\ & & \omega_{15} & & \omega_{18} & & \omega_6 & & \omega_7 \\ & & \rightarrow & R_5 & \rightarrow & R_2 & \rightarrow & R_3 & \rightarrow & f_1 \\ & & & & & & & & & \\ & & & & \omega_{16} & & & & & \\ & & & & \rightarrow & f_1 & & & & \end{array}$$

We have $\omega(R \rightarrow K_4 \rightarrow f_1) = \omega_{12} x \omega_{14} x \omega_6 x \omega_7 + \omega_{15} x \omega_{18} x \omega_6 x \omega_7 + \omega_{15} x \omega_{16} = 0.33[-10]$, and thus

$$\alpha^{\text{DR}}(R \rightarrow K_4 \rightarrow f_1) = 0.182[-19] \text{ cm}^3/\text{sec}. \quad (\text{A6})$$

(v) The state f_2 may be reached from K_4 by three different routes,

$$\begin{array}{ccccccc} \omega_{12} & & \omega_{13} & & & & \\ R & \rightarrow & K_4 & \rightarrow & f_2 & & \\ & & & & & & \\ & & \omega_{14} & & \omega_4 & & \omega_5 \\ & & \rightarrow & R_1 & \rightarrow & R_2 & \rightarrow & f_2 \\ & & & & & & & \\ & & \omega_{15} & & \omega_{18} & & \omega_5 \\ & & \rightarrow & R_5 & \rightarrow & R_2 & \rightarrow & f_2. \end{array}$$

Hence, $\omega(R \rightarrow K_4 \rightarrow f_2) = \omega_{12}(\omega_{13} + \omega_{14} x \omega_4 x \omega_5 + \omega_{15} x \omega_{18} x \omega_5) = 0.925[-7]$, and thus

$$\alpha^{\text{DR}}(R \rightarrow K_4 \rightarrow f_2) = 0.51[-16] \text{ cm}^3/\text{sec}. \quad (\text{A7})$$

(vi) The state f_3 may be generated from K_4 as

$$R \xrightarrow{\omega_{12}} K_4 \xrightarrow{\omega_{15}} R_5 \xrightarrow{\omega_{17}} f_3.$$

Hence we have $\omega(R \rightarrow K_4 \rightarrow f_3) = \omega_{12} x \omega_{15} x \omega_{17} = 0.302[-10]$ and so

$$\alpha^{\text{DR}}(R \rightarrow K_4 \rightarrow f_3) = 0.167[-19] \text{ cm}^3/\text{sec}. \quad (\text{A8})$$

Now the distribution of DR rates for the given $R = 2p^5 3d4s$ state on the final excited states can be obtained as follows: Add Eqs. (A3) and (A6) and obtain the DR rate for f_1 , $\alpha^{\text{DR}}(f_1) = 0.13[-18] \text{ cm}^3/\text{sec}$. Add Eqs. (A4) and (A7) and obtain the DR rate for f_2 , $\alpha^{\text{DR}}(f_2) = 0.55[-16] \text{ cm}^3/\text{sec}$. Add Eqs. (A2) and (A8) and obtain the DR rate for f_3 , $\alpha^{\text{DR}}(f_3) = 0.48[-14] \text{ cm}^3/\text{sec}$. Add Eqs. (A1) and (A5) and obtain the DR rate for f_4 , $\alpha^{\text{DR}}(f_4) = 2.41[-14] \text{ cm}^3/\text{sec}$.

When one of the earlier ω 's is small in a given chain of cascades, many simplifications can result. In the actual calculation presented in Tables I–V, many small contributions are neglected by truncating the cascade series.

-
- [1] Y. Hahn, Rep. Prog. Phys. **60**, 691 (1997).
[2] Y. Hahn, in Proceedings of the International Seminar on Atomic Processes in Plasmas, Tokyo, edited by T. Kato and I. Murakami [J. Quant. Spectrosc. Radiat. Transf. **49**, 81 (1993)].
[3] *Recombination of Atomic Ions* Vol. 296 of *NATO Advanced Study Institute, States of Physics*, edited by W. Graham, W. Fritsch, Y. Hahn, and J. A. Tanis (Plenum Press, New York, 1992).
[4] D. S. Belic, G. H. Dunn, T. J. Morgan, D. W. Muller, and C. Timmer, Phys. Rev. Lett. **50**, 339 (1983); A. Muller, D. S. Belic, B. D. DePaola, N. Djuric, G. H. Dunn, D. W. Muller, and C. Timmer, *ibid.* **56**, 127 (1986).
[5] B. A. Mitchell, C. T. Ng, J. L. Forand, D. P. Levac, R. E. Mitchell, A. Sen, D. B. Miko, and J. W. McGowan, Phys. Rev. Lett. **50**, 335 (1983).
[6] P. F. Dittner, S. Datz, P. D. Miller, C. D. Moak, P. H. Stelson, C. Bottcher, W. B. Dress, G. D. Alton, and N. Neskovic, Phys. Rev. Lett. **51**, 31 (1983).
[7] W. Zong, R. Schuch, E. Lindorff, H. Gao, D. R. Dewitt, and S. Asp, Phys. Rev. A **56**, 388 (1997).
[8] D. R. Bates, A. E. Kingston, and R. W. P. McWhirter, Proc. R. Soc. London, Ser. A **267**, 297 (1962).
[9] J. Li and Y. Hahn, Phys. Rev. E **48**, 2934 (1993); **49**, 927 (1994); **52**, 4281 (1995).
[10] D. B. Riesenfeld, Astrophys. J. **398**, 386 (1992).
[11] G. Omar and Y. Hahn, Phys. Rev. E **62**, 4096 (2000).
[12] G. Omar and Y. Hahn, Phys. Rev. A **37**, 1983 (1988).
[13] M. S. Pindzola, D. C. Griffin, and C. Bottcher, Phys. Rev. A **32**, 822 (1985).
[14] I. Nasser and Y. Hahn, J. Phys. B **25**, 521 (1992).
[15] I. Nasser and Y. Hahn, J. Korean Phys. Soc. **25**, 510 (1992).
[16] J. Li and Y. Hahn, Z. Phys. D **36**, 85 (1996); **41**, 19 (1997).